

## Anomaly in the dynamic behavior of the electroclinic effect below the nematic–smectic-*A* phase transition

Zili Li, Robert B. Akins, Gregory A. DiLisi, Charles Rosenblatt, and Rolfe G. Petschek

*Department of Physics, Case Western Reserve University, Cleveland, Ohio 44106*

(Received 23 July 1990)

The electroclinic effect and dielectric response have been investigated in the British Drug House material SCE12 over its entire 15-K smectic-*A* range. Near the smectic-*A*–smectic-*C*\*-phase transition both the electroclinic coefficient and dynamic response behave normally, the former diverging and the latter exhibiting a critical slowing down on approaching  $T_{A-C^*}$  from above. Similar behavior is seen in the dielectric response. Approximately 10 to 12 K above  $T_{A-C^*}$ , however, it was found that the electroclinic relaxation time levels off and even begins to increase again on approaching the nematic–smectic-*A* transition from below. The magnitude of the electroclinic coefficient, however, decreases monotonically on approaching the nematic–smectic-*A* transition.

The electroclinic effect in the smectic-*A* phase of a chiral liquid crystal was discovered by Garoff and Meyer in 1977.<sup>1,2</sup> In the lower-temperature smectic-*C*\* phase the molecules are tilted with respect to the layer normal and, being chiral, exhibit a spontaneous electric polarization perpendicular to the molecules and in the plane of the smectic layers. In the higher-temperature smectic-*A* phase one can apply an electric field parallel to the smectic layer plane which couples to the molecular dipole moment. The free energy associated with this electrostatic coupling ( $-\mathbf{E}\cdot\mathbf{P}$ ) competes with the cost of inducing a tilt above the smectic-*A*–smectic-*C*\* (Sm*A*–Sm-*C*\*) transition, resulting in an equilibrium molecular tilt  $\theta \propto E$ . This is the classical electroclinic effect.

One of the original problems associated with the electroclinic effect was the anomalous susceptibility critical exponent  $\gamma$ . Using the material *p*-decyloxybenzylidene-*p*'-amino-2-methylbutylcinnamate (DOBAMBC), Garoff and Meyer found a value  $\gamma = 1.11 \pm 0.06$ ,<sup>1,2</sup> inconsistent with either a mean-field value ( $\gamma = 1$ ) or a three-dimensional *XY* model ( $\gamma = 1.32$ ). In the intervening years other materials were studied by not only the classical electroclinic technique,<sup>3,4</sup> but using an indirect pyroelectric measurement as well.<sup>5</sup> The resulting exponents  $\gamma$  all tend to cluster on the slightly high side of the mean-field value, indicating that the discrepancy from  $\gamma = 1$  might be due to some material-dependent property. In this light Beresnev *et al.* suggested<sup>6</sup> that the anomalous behavior in  $\gamma$ , particularly in DOBAMBC, is due to a temperature-dependent coupling between the molecular dipole moment and the optically polarizable molecular core. Very recently this suggestion was verified by Li and Rosenblatt,<sup>7</sup> who performed an experiment on DOBAMBC involving crossed electric and magnetic fields. At a given temperature in the smectic-*A* phase they determined the ratio  $E/H^2$  required to maintain molecular orientation normal to the layers, finding that this ratio had a weak temperature dependence. Since this temperature dependence very closely mimics Garoff and

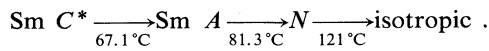
Meyer's result, and it is well known that  $d\theta/dH^2 \propto (T - T_{A-C^*})^{-1}$ , they concluded that the anomalous electroclinic susceptibility exponent is due to a temperature-dependent optical-dipolar coupling coefficient.

The dynamics associated with the Sm-*A*–Sm-*C*\* transition first came under scrutiny by Blinc and Zeks in 1978.<sup>8</sup> Much of the work since has centered on studies of the soft and Goldstone modes in the lower-temperature smectic-*C*\* phase. Levstik *et al.* for example, have resolved their dielectric data into contributions from each of the two modes.<sup>9</sup> Moreover, they have examined their results in terms of a Landau free energy, deriving expressions for these contributions in terms of other measurable parameters associated with the smectic-*C*\* phase. Dielectric studies of the soft and Goldstone modes have also been carried out by Bahr and Heppke in the presence of a dc electric field.<sup>4</sup> Their results indicate a temperature shift in the dielectric data, in agreement with previously reported shifts in  $T_{A-C^*}$ . These modes, as well as the soft mode in the smectic-*A* phase, have also been examined by means of quasielastic light scattering by Drevensek *et al.*<sup>10</sup> They obtained both the temperature dependence and dispersion relationships for these modes, finding that in the smectic-*C*\* phase the soft mode relaxation time is temperature dependent, whereas the Goldstone time is independent of temperature.

Although these studies have revealed considerable information about the smectic-*A*–smectic-*C*\* phase transition and associated director modes, apparently no study to date has investigated the dynamics of the soft mode in the smectic-*A* phase near the nematic transition. Even investigations of the nematic–smectic-*A*–smectic-*C* multicritical point have centered on issues near transitions to the smectic-*C* phase (from both the nematic and smectic *A*), rather than on the behavior of smectic-*C*-like fluctuations near the nematic–smectic-*A* transition. Examination of the changes in the electroclinic effect near the

Sm-*A*–nematic transition are of interest for a variety of reasons. For example, there is no reason of symmetry why the electroclinic effect should fundamentally change with the disappearance of long-range translational order at the nematic–smectic-*A* transition. Since microscopic correlations between the positions of the molecules change rapidly with temperature in the vicinity of this transition, one can experimentally assess the importance of translational order on the electroclinic effect. With this in mind we have performed both optical (electroclinic) and dielectric studies of the smectic-*C* soft mode over the entire smectic-*A* phase of a ferroelectric liquid crystal.

We studied the material SCE12, which was kindly supplied to us by BDH Ltd. through EM industries. This multicomponent mixture was used as is. SCE12 is a compensated mixture with a pitch many tens of micrometers over a temperature range several degrees above  $T_{N-A}$ ; the transition temperatures are given approximately as



For the electroclinic studies, the material was inserted between a pair of indium tin oxide–coated glass microscope slides, which had been treated with the polymer nylon 6/6 and rubbed to give homogeneous orientation, i.e., the bookshelf geometry. The sample spacing was nominally 25  $\mu\text{m}$ , as determined by a pair of Mylar spacers. Prior to the experiment the sample was checked by means of an optical polarizing microscope so as to determine the quality of the alignment; the sample was found to be defect-free and well aligned. The sample was then housed in a well-insulated brass oven temperature controlled to approximately 1.5 mK by a YSI model 72 controller. Unlike previous experiments,<sup>11</sup> the laser beam was unfocused, and we therefore estimate that the temperature gradient across the illuminated region was less than 15 mK.

Details of the optical and detection apparatus can be found in Refs. 11 and 12. Briefly, the beam, from a He-Ne laser attenuated to approximately 0.1 mW, was directed along the *x* axis in the laboratory frame, and passed consecutively through a Glan-Thomson polarizer oriented at an angle 22.5° from the *z* axis, the sample, a crossed polarizer, and into the detector. The detector output was fed into both a Keithley model 196 digital voltmeter for measurements of the dc intensity and a Stanford Research SR530 two phase lock-in amplifier for measurements of the ac component of intensity. If an ac voltage  $V(\omega)$  is applied to the electrodes, thereby inducing a tilt  $\theta$ , one can easily show for this geometry that

$$\theta = \delta I / 4I_0 , \quad (1)$$

where  $\delta I$  is the intensity at frequency  $\omega$  as measured by the lock-in amplifier, and  $I_0$  is the dc intensity. If, however, a rapidly varying voltage is applied to the electrodes, one expects a phase delay in  $\theta$  relative to the applied voltage, as well as a reduction in the magnitude of  $\theta$ . Assuming a Debye (i.e., Lorentzian) process described by a single relaxation time, we can write a simple differential equation for  $\theta$ :

$$\eta \frac{d\theta}{dt} + C^{-1}\theta = E , \quad (2)$$

where  $\eta$  is a kinetic coefficient,  $C$  the temperature-dependent electroclinic coefficient  $d\theta/dE$  at frequency  $\omega=0$ , and  $E$  the applied electric field. For  $E = E_0 \cos \omega t$ ,  $\theta$  is given by

$$\theta = \frac{CE_0}{1 + \omega^2\tau^2} (\cos \omega t + \omega\tau \sin \omega t) \quad (3)$$

where the relaxation time  $\tau = C\eta$ . Thus, by measuring the ratio  $R$  of the in-phase component of  $\theta$  to its out-of-phase component, one finds that  $\tau = 1/R\omega$ .

For each temperature in the smectic-*A* phase, the in-phase and  $\pi/2$  out-of-phase (quadrature) components of  $\theta$ , viz.,  $\theta_{\text{in}}$  and  $\theta_{\text{out}}$ , were measured at three different frequencies as a function of applied field from  $E=0$  through  $E=4 \times 10^5$  V/m. The (angular) frequencies  $\omega$  were chosen such that  $1/\omega$  was approximately one-third, two-thirds, and equal to the apparent relaxation time  $\tau$ . For each frequency,  $\tau$  was determined from the relationship  $\tau = \theta_{\text{out}}/\omega\theta_{\text{in}}$ , where the three relaxation times were found to be in good agreement (within 10–15% of each other). Figure 1 shows the relaxation time versus temperature, where for consistency we display the data at the lowest frequency used for each temperature. (We note that it was necessary to correct the raw data for the finite response time of the detector, which was determined to be 100 ns. For large  $\tau$ , where slower driving frequencies were used, this correction is negligible; for the fastest response times requiring the highest frequencies, the correction is about 5%, smaller than the size of the data point itself.) Figure 2 shows the dc electroclinic coefficient  $C$ , which can be extracted from Eq. (3) once the temperature-dependent response time  $\tau$  is obtained.

As is obvious from Fig. 1, the response time appears to diverge near  $T_{A-C^*}$ . What is unexpected, however, is the cusplike anomalous slowing down of the electroclinic response beginning about 10 K above the smectic-*A*–smectic-*C*\* transition, a behavior very different from that described in Ref. 4. This result is even more perplex-

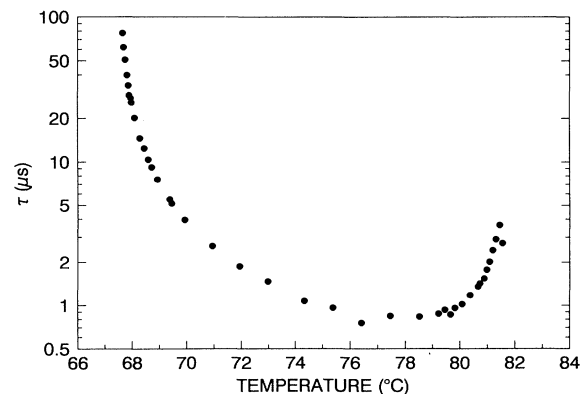


FIG. 1. Apparent response time of electroclinic effect vs temperature. Last point is in the nematic phase. Error bars are comparable to the size of the data points.

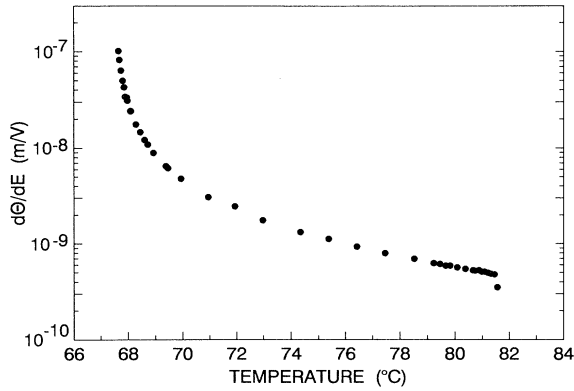


FIG. 2. Magnitude of the electroclinic coefficient  $C$  ( $\equiv d\theta/dE$ ) vs temperature. Last point is in the nematic phase.

ing in light of the dc electroclinic results in Fig. 2, i.e., no apparent anomalous behavior is observed in  $C$  on approaching  $T_{N-A}$ . Given these two sets of data, it is difficult to imagine a scenario in which mode coupling to layer fluctuations near  $T_{N-A}$  drives the anomaly. It is thus apparent that additional data, probing only the electrical response, are necessary; to that end we have also performed dielectric measurements on SCE12. Since frequencies up to  $f=1$  MHz were to be used (where  $f=\omega/2\pi$ ), semitransparent gold electrodes were evaporated onto a pair of glass slides, then rubbed to give homogeneous alignment. The glass was then placed together to form a cell approximately  $60 \mu\text{m}$  thick. Using optical microscopy, the overlap area of the electrodes was determined, and by measuring the empty cell capacitance (using a Hewlett-Packard model 4284A precision LCR meter operating at 1 V), the cell spacing was determined to be  $d=59.7\pm 0.3 \mu\text{m}$ . The cell was then loaded with SCE12, and the complex dielectric constant was measured for frequencies  $10^3 < f < 10^6$  Hz at temperatures throughout the entire smectic- $A$  range. Figure 3 shows the imaginary part of the dielectric constant  $\epsilon$  at six selected temperatures over the frequency range for which  $\text{Im}(\epsilon)$  exhibits a peak. Below 10–20 kHz (not easily observable in Fig. 3) there is a component to the dispersion arising from low-frequency (dc) conductivity. This component was fitted using standard procedures<sup>13</sup> and subtracted from the raw data. The resulting data have a low-frequency (slow) peak which increases in frequency with increasing temperature. In addition, at higher temperatures, the low-frequency tail of a higher-frequency (fast) peak is observable, and for sufficiently high temperatures, this tail eventually dominates the slow peak. The data were then fitted assuming two separate peaks to the semiempirical Fuoss-Kirkwood model for dielectric relaxation:<sup>14</sup>

$$\text{Im}(\epsilon) = \sum_j A_j \text{sech}[b_j \log_e(\omega/\Omega_j)], \quad (4)$$

where  $A$ ,  $b$ , and  $\Omega$  are temperature-dependent fitted parameters and the index  $j$  refers to the slow or fast peak.

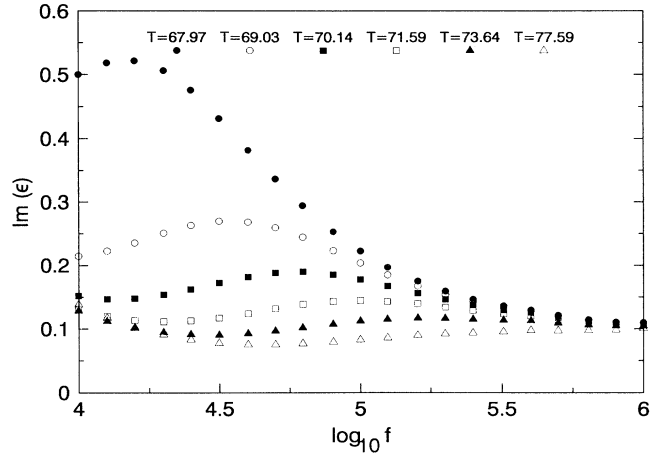


FIG. 3. Imaginary part of the dielectric constant vs frequency  $f$  ( $\equiv \omega/2\pi$ ) at several temperatures in the smectic- $A$  phase.

This model is essentially a broadened Debye model for dielectric relaxation, arising from a number of considerations such as a distribution of relaxation times and activation energies, as well as the inclusion of dipole-dipole interactions. Our apparatus does not currently allow us to go to high enough frequencies to find the maximum in the high-frequency peak anywhere in this temperature range. In consequence the high-frequency peak was fitted by choosing a fixed relaxation frequency of  $10^8$  Hz and  $b=0.7$ . Since the tail portion of a Fuoss-Kirkwood peak is quite insensitive to considerable variations in these parameters, other choices of parameters would have given essentially the same results over frequencies below  $10^6$  Hz. It was found that the low-frequency peak is well approximated by an unbroadened Debye peak over the whole smectic- $A$  range, analogous to Ref. 4.

Figure 4 shows the product of  $\omega_s \tau$ , where  $\omega_s$  is the re-

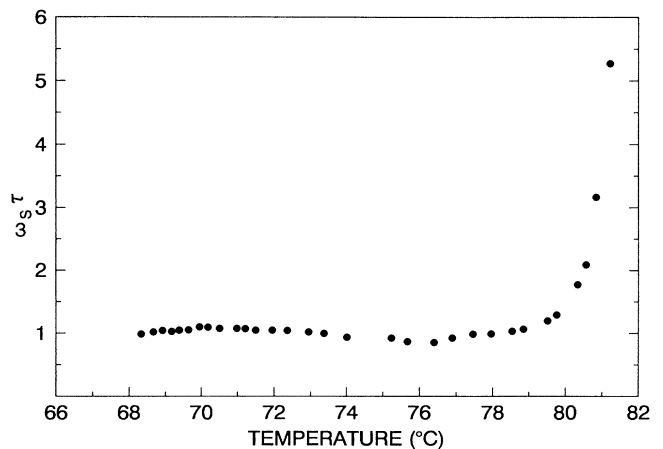


FIG. 4.  $\omega_s \tau$  vs temperature, where  $\omega_s$  is the frequency of the slow dielectric peak and  $\tau$  is the apparent relaxation time of the electroclinic effect.

laxation frequency obtained for the slow peak and  $\tau$  is the relaxation time obtained from the electroclinic measurements above. Over the smectic- $A$  range, except very close to the  $N$ -Sm- $A$  transition, this product is equal to unity, indicating that the low-frequency dielectric peak corresponds to the usual electroclinic process. (Different ovens and thermometers were used for the optical and dielectric measurements. So as to compensate for a difference in their absolute temperature scales, the temperature for the electroclinic data was shifted by 0.34 °C.) At high temperatures, however, the product  $\omega_s \tau$  clearly deviates from unity, independent of any temperature shift; this issue is related to the anomalous behavior in the electroclinic coefficient  $C$ , and will be addressed below.

Finally, we have performed a Kramers-Kronig calculation using the dielectric loss data in the low-frequency peak. The resulting real part of the susceptibility  $\chi'(0) \equiv dP/dE|_{f=0}$  was obtained, and its inverse is plotted versus temperature along with  $C^{-1}$  in Fig. 5. Note that the polarization  $P$  corresponds solely to the ferroelectric transverse dipole moment: since  $\chi'$  was obtained using a Kramers-Kronig formulation, we have chosen to include contributions to the polarizability from the low-frequency loss peak only, as determined from the fit in Eq. (4). Thus both the normal electronic contribution to the real part of the polarizability, and higher-frequency molecular reorientations (e.g., those responsible for the high-frequency loss in our dielectric measurements) are excluded from  $\chi'$ .

In order to understand the results we begin by writing the free energy  $g$  associated with the smectic- $A$ -smectic- $C^*$  phase transition. Adopting the notation of Ref. 1, we find

$$g = g_A + \frac{1}{2} A'(T) \theta^2 + O(\theta^4) + \frac{1}{2} \chi_P^{-1} P^2 - PE - 8\pi\epsilon^0 E^2 - t\theta P.$$

$P$  is the component of polarization parallel to  $E$ ,  $\epsilon^0$  the dielectric constant in the absence of a permanent dipole,  $\chi_P$  the generalized susceptibility, and  $t$  is the coefficient coupling  $\theta$  and  $P$ . Since  $P$  and  $\theta$  are treated as indepen-

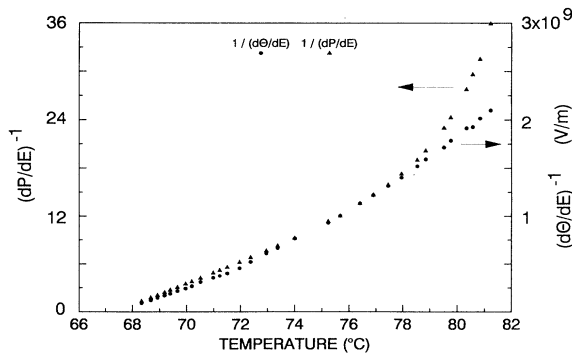


FIG. 5. Inverse susceptibility  $\chi'^{-1} [\equiv (dP/dE)^{-1}]$  and inverse electroclinic coefficient  $C^{-1} [\equiv (d\theta/dE)^{-1}]$  vs temperature.

dent variables,  $g$  must be minimized with respect to both. In the static case, we find that  $\theta = tE\chi_P/A(T)$ , where  $A(T) = A'(T) - \chi_P t^2$ . Note that the dc electroclinic coefficient is  $C = t\chi_P/A(T)$ . The susceptibility  $\chi_P$  is expected to be nearly constant and the coupling coefficient  $t$  is likely to be a weakly decreasing function of temperature. Since  $A'(T)$  scales as  $T - T_{A-C^*}$ , the end result is that  $C$  is a monotonically decreasing function of temperature, as seen in Fig. 2.

We now turn our attention to the temporal behavior of the system, where it is useful to examine a possible set of dynamical equations. We assume that the dynamic coefficients are unaffected by the chirality. Additionally, we assume that they do not depend strongly on the temperature. This might seem to be a risky assumption in view of the fact that various viscosities are known to diverge in the smectic- $A$  phase (and are presumed to diverge in the smectic- $C$  phase<sup>15</sup>) essentially because of the coupling between the velocity field and the slow, large layer undulation modes. Unfortunately a detailed treatment of the dynamics of the smectic- $A$  phase in which a tilt is included does not seem to be detailed in the literature, although the equations of motion have been given.<sup>16</sup> It is not our intention in this paper to give such a detailed treatment. We remark, however, that there is an appreciable difference between the tilt and the velocity in that the time derivative for uniform tilt is proportional to the tilt itself; thus layer undulations cannot directly result in a tilt. On the other hand, layer undulations in the absence of a velocity gradient can result in a velocity gradient. This completely changes the graphs which contribute to the modification of the associated dynamical constants. While we have not examined all possible graphs for the dynamics of the tilt, those which we have analyzed do not suggest that the tilt-related dynamic coefficients depend strongly on the layer undulation modes. Such a dependence might be important even if it did not result in a divergent viscosity, as it might cause a strong dependence of the dynamic coefficients on the elastic (and dynamic) coefficients of the smectic- $A$  phase, which change rapidly near the smectic- $A$ -nematic transition. With this reservation we suppose that the dynamic coefficients of the tilt do not vary quickly and consider the equations

$$\eta_P \frac{dP}{dt} = \frac{dg}{dP}, \quad (5a)$$

$$\eta_\theta \frac{d\theta}{dt} = \frac{dg}{d\theta}. \quad (5b)$$

In a chiral system like this, in principle it is also possible for there to be an off-diagonal term in these equations, for example, a term  $\eta_{P\theta} d\theta/dt$  on the left-hand side of Eq. (5a) and  $\eta_{P\theta} dP/dt$  on the left-hand side of Eq. (5b). However, these terms vanish in a nonchiral system and inclusion of these terms, provided  $\eta_{P\theta}^2 \lesssim \eta_P \eta_\theta$ , does not significantly alter the results. Since explicitly chiral terms are generally small in liquid crystals, we will thus ignore  $\eta_{P\theta}$  and will only discuss the simpler version of Eqs. (5a) and (5b) in what follows.

To calculate the frequency-dependent susceptibility we simply insert the assumption that  $P = P(\omega)e^{i\omega t}$ ,  $\theta = \theta(\omega)e^{i\omega t}$ , and  $E = E(\omega)e^{i\omega t}$ . This becomes an overdamped eigenvalue problem with a slow and fast decay, such that the tilt and dielectric responses can be expressed as linear combinations of these two modes. After some algebra we find that

$$\chi_{\theta E} = \left[ \frac{t\chi_P}{A} + \delta_\theta \right] \frac{1}{i\omega\tau_s + 1} - \delta_\theta \frac{1}{i\omega\tau_f + 1} \quad (6a)$$

where

$$\delta_\theta = \frac{t\tau_f^2}{\eta_\theta\eta_P} \frac{1}{1 - \tau_f/\tau_s}$$

and

$$\chi_{PE} = (\chi_P + \delta_P) \frac{1}{i\omega\tau_f + 1} + \left[ \frac{t^2\chi_P^2}{A'} - \delta_P \right] \frac{1}{i\omega\tau_s + 1} \quad (6b)$$

where

$$\delta_P = \chi_P \frac{1}{1 - \tau_f/\tau_s} \left[ 2 \left[ \frac{\tau_f}{\tau_s} - \frac{\tau_f A}{\eta_\theta} \right] - \left[ \frac{\tau_f A}{\eta_\theta} \right]^2 \right].$$

In Eqs. (6a) and (6b) the quantities  $\chi_{\theta E}$  and  $\chi_{PE}$  correspond to the complex susceptibilities  $d\theta/dE$  and  $dP/dE$ , respectively. Provided the slow relaxation is much slower than the fast relaxation ( $\tau_s \gg \tau_f$ , such that  $\delta_\theta$  and  $\delta_P$  are small corrections), we see that most of the tilt will relax at the slow rate and most of the polarization will relax at the faster rate. In effect, only that part of the polarization which is a response to the slowly relaxing part of the tilt will also relax at the slower rate. In Ref. 4 Bahr and Heppke observed only the slow component of the dielectric response; presumably the fast component was too small and/or too fast to observe. From Eqs. (6a) and (6b) it is thus expected that the area under the slower dielectric peak (corresponding to  $dP/dE$ ) should be nearly proportional to the electroclinic coefficient  $d\theta/dE$  over most of the smectic- $A$  range (cf. Fig. 5). A wide variety of ratios involving the amplitude of and relaxation rates for the dielectric and electroclinic data can be formed. With the exception discussed below, ratios in which the rapidly varying variables  $A$  and  $A'$  do not appear remain relatively constant throughout the nematic range.

Based upon our initial assumptions leading to Eqs. (6a) and (6b), it is expected that the experimental line shapes of the relaxation processes should be essentially Lorentzian; this is confirmed by the dielectric fit of the slow frequency peak. However, we were unable to collect electroclinic data at sufficiently high frequencies to unambiguously determine if the line shape is a sum of Lorentzians, where the slower process is dominant. As mentioned earlier, there do appear to be small (15%) indications of deviations from Lorentzian behavior.

It is also expected from these equations (and on quite general physical grounds for linearly coupled responses) that the relaxation rate associated with the low-frequency peak in the dielectric behavior and that associated with

the major relaxation in the electroclinic response are the same. Such behavior was observed in Ref. 4. Near the nematic transition, however, this is not observed in our data. While it is true that at these temperatures the slow electroclinic relaxation in the dielectric response is overwhelmed by the tail of the fast process and therefore difficult to fit accurately, attempts to fit it with the observed electroclinic relaxation rate were completely unsuccessful and appreciably decreased the quality of the fit.

Instead we choose a different approach. We note that  $\chi_{\theta E}$  is the difference between two susceptibilities. At lower temperatures, where both  $\delta_\theta$  and  $A'$  are small, the first (slow) term in Eq. (6a) is dominant. As discussed above,  $\tau$  is simply  $1/R\omega$ , where  $R$  is the ratio of the real to imaginary component of  $\theta$ . At higher temperatures, however, the second term in Eq. (6a) becomes important; the experimental ratio  $R$  then represents a combination of two processes, yielding an *effective* relaxation time  $\tau$  for the tilt  $\theta$ . (Note that even though the *ratio* may be nonmonotonic with temperature, the magnitude of the real component decreases monotonically with  $T$ , consistent with the data in Fig. 2.) Physically, this scenario corresponds to a two-step relaxation process beginning with a tilt  $\theta_0$  at time  $t=0$ . First, owing to the minus sign in Eq. (6a), the tilt of the molecule would increase by a small amount very rapidly; this corresponds to the fast process. The slow relaxation, approximately corresponding to the usual soft mode, would then take over, and the tilt angle would relax back to  $\theta=0$ . The apparent relaxation rate would appear slower than a process in which only a single slow mechanism were operative.

So as to determine whether the theoretical effective time can, in fact, increase on increasing the temperature toward  $T_{N-A}$  we note that  $\chi_{PE}$  can be written in the form

$$\chi_{PE} = \frac{a}{i\omega\tau_s + 1} + \frac{b}{i\omega\tau_f + 1} \quad (7a)$$

where  $a$  and  $b$  are coefficients given by Eq. (6b). We then form a linear combination of the two terms in the dielectric susceptibility to obtain the tilt susceptibility

$$\chi_{\theta E} = \alpha \left[ \frac{a}{i\omega\tau_s + 1} - \frac{A_2 b}{i\omega\tau_f + 1} \right] \quad (7b)$$

where  $\alpha$  is a scale factor which accounts for units and magnitude, and  $A_2$  is a factor which accounts for the differences in the peak heights. The minus sign in Eq. (7b) corresponds to the minus sign in Eq. (6a). Comparing Eq. (7b) with (6a) and (6b), we note that  $A_2$  is given by

$$A_2 \approx \frac{t^2\chi_P}{A'} \frac{\tau_f}{\tau_s} + O(\tau_f/\tau_s)^2. \quad (8)$$

We then form the ratio  $R$  of the real to imaginary part of Eq. (7b) and extract an effective relaxation time  $\tau_{\text{eff}} = 1/R\omega$ . By fixing  $\tau_f$ , using the experimental value of  $\tau_s$ , and adjusting  $\alpha$  and  $A_2$ , we find that  $\tau_{\text{eff}}$  can mimic the shape of a substantial portion of the experimental curve  $\tau$  versus  $T$  (cf. Fig. 1), including the apparent relaxation time increase above  $\sim 79^\circ\text{C}$ . It turns out that the

best "fits" are obtained for  $A_2 \sim 0.1$  to 0.15, although it must be noted that substantial (>50%) deviations from the experimental values of  $\tau$  occur within 1 K of  $T_{N-A}$ .

In Eq. (8) the quantity  $i^2\chi_p/A'$  corresponds to  $\Delta T_{A-C^*}/(T-T_{A-C^*})$ , where  $\Delta T_{A-C^*}$  is the shift in the smectic- $A$ –smectic- $C^*$  transition temperature arising from chirality. We therefore might expect  $A_2$  to be  $\sim 0.1\tau_f/\tau_s$ .<sup>17</sup> Since  $A_2$  was also determined to be of order 0.1, we would expect the fast and slow processes to have approximately the same relaxation times; this is obviously not so. Moreover, contrary to the predictions of Eq. (7b), we experimentally find that the relaxation can be described to within approximately 15% by a single Lorentzian, and *improves* on approaching  $T_{N-A}$ . Taken together, these considerations indicate that the mechanism is likely to be considerably more complex than that outlined above.

In conclusion, we have measured the optical electro-

clinic relaxation time throughout the smectic- $A$  range in a multicomponent mixture. Two dielectric processes were also measured, where the slower dielectric process corresponds to that observed optically over most of the smectic- $A$  range. For  $T > T_{A-C^*} + 10$  K, however, the optical relaxation time begins to increase on increasing temperature, in contrast to the behavior of the slower dielectric peak. An attempt was made fit a linear combination of the two dielectric processes to the optical data, with marginal success. At this time, then, a search is being conducted to find other materials with much simpler compositions in order to systematically investigate the origins of this anomaly.

This work was supported by the National Science Foundation under Grants No. DMR-8901845 and No. DMR-8796354. The authors are indebted to Dr. Frank Allan for the SCE12.

<sup>1</sup>S. Garoff and R. B. Meyer, Phys. Rev. Lett. **38**, 848 (1977).

<sup>2</sup>S. Garoff and R. B. Meyer, Phys. Rev. A **19**, 338 (1979).

<sup>3</sup>R. Qiu, J. T. Ho, and S. K. Hark, Phys. Rev. A **38**, 1653 (1988).

<sup>4</sup>Ch. Bahr and G. Heppke, Liq. Cryst. **2**, 825 (1987).

<sup>5</sup>E. P. Pozhidayev, L. M. Blinov, L. A. Beresnev, and V. V. Belyayev, Mol. Cryst. Liq. Cryst. **124**, 359 (1985).

<sup>6</sup>L. A. Beresnev, L. M. Blinov, M. A. Osipov, and S. A. Pikin, Mol. Cryst. Liq. Cryst. **158A**, 3 (1988).

<sup>7</sup>Z. Li and C. Rosenblatt, Phys. Rev. A **39**, 1594 (1989).

<sup>8</sup>R. Blinc and B. Zeks, Phys. Rev. A **18**, 740 (1978).

<sup>9</sup>A. Levstik, T. Carlsson, C. Filipic, I. Levstik, and B. Zeks, Phys. Rev. A **35**, 3527 (1987).

<sup>10</sup>A. Drevensek, I. Musevic, and M. Copic, Phys. Rev. A **41**, 923 (1990).

<sup>11</sup>Z. Li, G. A. DiLisi, R. G. Petschek, and C. Rosenblatt, Phys.

Rev. A **41**, 1997 (1990).

<sup>12</sup>Z. Li, R. G. Petschek, and C. Rosenblatt, Phys. Rev. Lett. **62**, 796 (1989); **62**, 1577(E) (1989).

<sup>13</sup>N. G. McCrum, B. E. Read, and G. Williams, *Anelastic and Dielectric Effects in Polymeric Solids* (Wiley, New York, 1967).

<sup>14</sup>R. M. Fuoss and J. G. Kirkwood, J. Am. Chem. Soc. **63**, 385 (1941).

<sup>15</sup>G. F. Mazenko, S. Ramaswamy, and J. Toner, Phys. Rev. A **28**, 1618 (1983).

<sup>16</sup>E. V. Gurovich, E. I. Kats, and V. V. Lebedev, Zh. Eksp. Teor. Fiz. **94**, 167 (1988) [Sov. Phys.—JETP **67**, 741 (1988)].

<sup>17</sup>S. Garoff, Ph.D. thesis, Harvard University, 1977 (unpublished).